Space Sci Rev (2012) 171:85–95
DOI 10.1007/s11214-011-9742-7

The Time Structure of Ground Level Enhancements in Solar Cycle 23

H. Moraal · K.G. McCracken

Received: 17 May 2010 / Accepted: 31 December 2010 / Published online: 24 February 2011

Abstract In a recent paper McCracken et al. (J. Geophys. Res. 113:A12101, 2008) proposed that the Ground Level Enhancement (GLE) of 20 January 2005 may have been produced by more than one acceleration mechanism, with the first acceleration due to the solar flare and the second one due to the CME associated with that event. They also noted several other GLEs with similar multiple pulse structures. This paper systematically investigates all the GLEs of solar cycle 23, from GLE 55 on 6 November 1997 to GLE 70 on 13 December 2006, to study their morphology and pulse structure, and to determine whether the multiple structures that may be found in these events are qualitatively similar to that of the GLE of 20 January 2005. We use all the data of all NMs that saw each event, to have as much directional and spectral information as possible. It is shown that three of these 16 events do contain such double-pulse structures, and the properties of these three are discussed in some detail.

Keywords Solar cosmic rays · Ground level enhancements · Neutron monitors · Solar Flares · Coronal mass ejections

1 Introduction

Seventy so-called ground level enhancements (GLEs) have been recorded since 1942, mainly by the worldwide network of neutron monitors (NMs). These GLEs are at the high-energy end of the solar energetic particle (SEP) spectrum, and hence they represent the strongest acceleration episodes on the sun. NMs are particularly well-suited to record these GLEs because their high counting rate leads to high statistical significance of the increases, and excellent directional sensitivity can be achieved by considering the increases seen by all 40-odd NMs together.

H. Moraal (✉)
Unit for Space Physics, North-West University, Potchefstroom 2520, South Africa
e-mail: harm.moraal@nwu.ac.za

K.G. McCracken
Institute for Physical Science and Technology, University of Maryland, College Park, MD, 20742, USA

Originally, the source of SEPs was ascribed to acceleration in solar flares, but during the last approximately 25 years the consensus has formed that the bulk of the acceleration is due to stochastic first-order Fermi acceleration by the bow shock of the coronal mass ejection (CME) that often accompanies such a flare event. The field is described in e.g. Von Rosenvinge and Cane (2006) and Cliver (2008).

McCracken et al. (2008) (hereinafter called Paper 1) proposed, however, that GLE number 69 on 20 January 2005 may have been produced by more than one acceleration mechanism, with the first one likely being the solar flare, and the second one the CME shock. The arguments were mainly based on the promptness and strong anisotropy of the first pulse (P1), as opposed to a much less anisotropic and more gradual second pulse (P2). We note that hitherto double pulses in GLEs have been mainly attributed to propagation effects in the heliospheric magnetic field (HMF), e.g. by Bieber et al. (2002, 2004, 2007) and Saiz et al. (2008).

The case for a double acceleration mechanism was further supported by a sudden (within one minute) softening of the spectrum as seen by the combination of the Sanae NM and neutron moderated detector (NMD; a neutron monitor without lead producer). These two detectors have different energy responses, and their combination was unique for this event because they saw the two pulses with roughly the same size, so that the one pulse was not submerged by the other, as happened with most NMs. Paper 1 also noted that 10 out of the 22 large ($> 20\%$) GLEs in the historic record showed indications of similar double-pulse structures, but a detailed analysis on these events has not yet been done.

The purpose of this paper is to start such an analysis by systematically investigating the 16 GLEs of solar cycle 23 (SC 23) for double-peak structures, and describe them in detail. We do this by first reviewing the main points of evidence for a double-peak structure we found in Paper 1 for GLE 69, and we then extend this to the others. A preliminary version of this work can be found in Moraal and Reinecke (2009).

2 The GLE of 20 January 2005

The two panels of Fig. 1 show the first and second pulses that we identified in Paper 1 for GLE 69 on 20 January 2005. The first peak was prompt, it started at $\approx$ 06:49, and peaked at 06:54. All times mentioned in this paper are Earth observation time in UT. The largest increase of 80 times (8000%) was seen at South Pole, and this places the GLE as the second largest one on record, after GLE 5 of 23 February 1956.

The second pulse was qualitatively different, being much smaller, much more gradual in its rise time, and it also lasted much longer. It started 5 minutes after P1, and peaked at 07:06. A few stations saw a combination of the two pulses. They are the Sanae NM and NMD, as well as Fort Smith and, possibly, Newark.

Paper 1 presented the following points of evidence for two separate source mechanisms for the two pulses.

1. Anisotropy. Of the 28 neutron monitors that saw the GLE, only nine recorded the first pulse P1. Paper 1 showed that these detectors had asymptotic cones of direction around a direction 85° South and 40° West, and that this direction of symmetry agreed with the direction of the heliospheric magnetic field (HMF) during the event. Thus P1 was identified as a highly anisotropic beam with the particles strongly collimated along the HMF. On the other hand, pulse P2 was observed by many more NMs, and the bottom panel of Fig. 1 shows that the differences in amplitude were much smaller than during P1, which indicates that the anisotropy was much smaller. The anisotropy was, in fact, significantly smaller

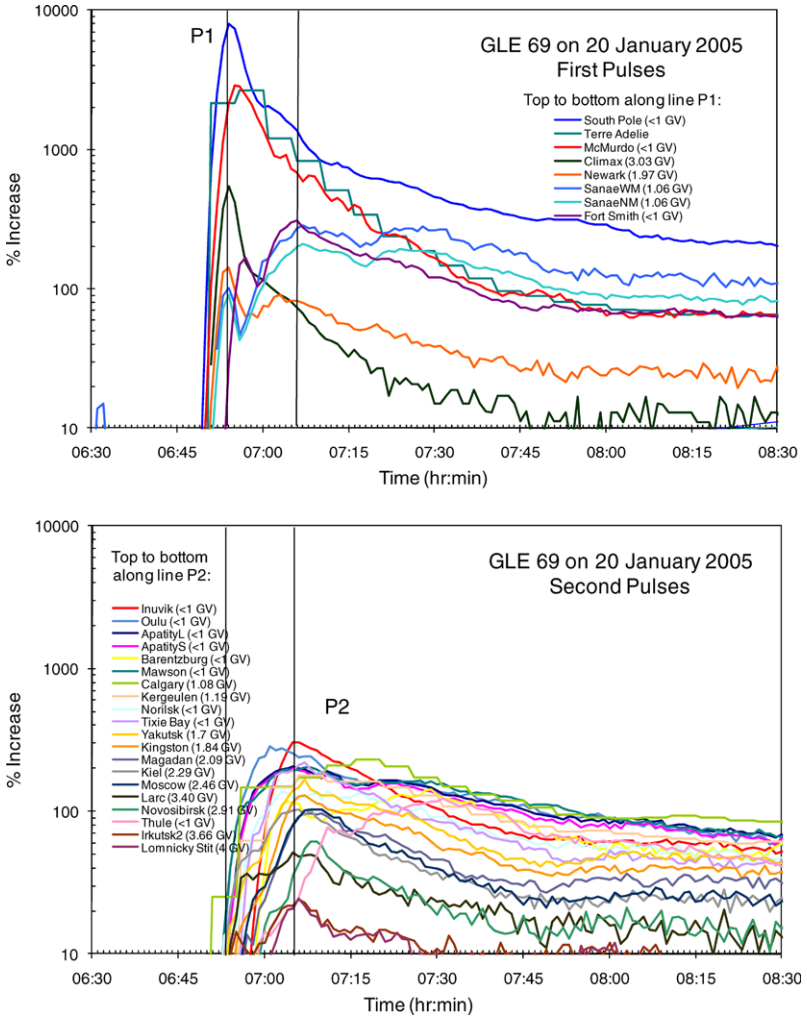

Fig. 1 Ground Level Enhancement 69 of 20 January 2005. The *top panel* shows the first, prompt pulse P1, while the *lower panel* shows the second, more gradual pulse P2. The *lines* P1 and P2 mark the time of maximum of each of the pulses. The *legend* gives the cutoff rigidity P_c of each station in GV. For polar NMs the geomagnetic cutoff is lower than the atmospheric cutoff of 1 GV. The *top panel* shows that the Sanae NM and NMD, as well as the Fort Smith and Newark NMs saw both P1 and P2

right from the early phases of P2, which favors that this pulse was produced by a more isotropic injection/acceleration mechanism than P1. We note that the conservation of the longitudinal adiabatic invariant, $\sin^2\theta/B$, naturally favors a stronger anisotropy for particles produced near the surface of the sun. For a field that falls off as $1/r^2$, it leads to the condition $r_1 \sin\theta_1 = r_2 \sin\theta_2$. Hence, particles that are produced in a flare at approximately one solar radius, will already be strongly focused when they reach the typical radius of 5 to 10 solar radii where CME shock acceleration happens once the shock has formed.

2. Spectral index. During the short-duration pulse P1, the increase on the Sanae NM and Sanae NMD were similar. However, Figure 2 of Paper 1 shows that at the start of the

extended P2, the increase in the NMD rate suddenly (within 2 minutes) rose above that of the NM, and the NMD/NM ratio remained high during the remainder of the event. Since the NMD has a response function that favors low-energy particles more than the NM, this indicates that during P2 the spectrum was significantly softer than during P1.

3. Promptness. Pulse 1 had a rate of increase at its leading edge of $\sim$ 1600%/min., which is the fastest rise ever seen in a GLE. On the other hand, P2 had a much more moderate increase rate of $\sim$30%/min., which is characteristic of many other GLEs. Fast (slow) rise times are characteristic of weak (strong) scattering during propagation. However, the time interval between the two pulses is so short, $\approx$10 min., that one does not expect the HMF to change its turbulence properties on such a short time scale. Thus, this suggests different source mechanisms for the two pulses, rather than different transport effects.

4. Velocity dispersion in P1. The two panels of Fig. 1 show that the onset dispersion in P1 is significantly smaller than that in P2. For P1, only Fort Smith lags significantly behind the other NMs, and in Paper 1 we could explain this lag as due to the fact that Fort Smith was the only detector in this group that observed particles with speed significantly less than c. For the other NMs it is not only the onset time that agrees well, but the time of the peak intensity agrees even better. In Figure 6 of Paper 1 we showed that the time of the peak of P1 for the Grand muon telescope (cutoff rigidity $P_c = 11$ GV, the Milagro Cerenkov detector, $P_c = 4$ GV, and the Climax and Sanae neutron monitors, $P_c = 2.4$ and 0.8 GV respectively, are all the same, within the time resolution of 1 minute. We also showed that the Sanae NM had its asymptotic cone of viewing so directed that it could only have seen the high-energy tail of P1, well above the cutoff rigidity of 0.8 GV. Thus, these four detectors all saw relativistic particles with speed essentially equal to c, which means that they should have had nearly the same propagation time, and this implies that they were accelerated at the same time.

An acceleration time scale to energies that differ by more than a factor of 5 to 10 is not possible with first-order Fermi (or shock) acceleration, where the acceleration time scale is κ/V^2, where κ is the diffusion coefficient and V the solar wind speed. The relationship between diffusion coefficient and diffusion mean free path is $\kappa = v\lambda/3$, and according to Caballero-Lopez et al. (2004) the typical mean free path at Earth that fits the galactic cosmic ray modulation is $\lambda = 0.25P$ (GV) AU. This leads to an acceleration time scale of $260\beta P$ (GV) days (where $\beta = v/c$). Diffusion coefficients should scale approximately inversely proportional to B, and in the inner heliosphere the Parker spiral field scales as $1/r^2$. Thus the acceleration time scale at 3 solar radii is $\approx 1\beta P$(GV) hr. The observations mentioned above do not support an acceleration time that increases with increasing cutoff rigidity, and the magnitude is also too long. We note, however, that this estimate is highly uncertain, and that it may be significantly reduced through self-excitation of waves, as calculated by e.g. Ng and Reames (2008).

5. Velocity dispersion in P2. In contrast, the bottom panel of Fig. 1 shows that for P2 the situation is different, with a spread of up to 10 minutes in the start times and peak times. The legend on this panel draws attention to the fact that the increases at stations with a geomagnetic cutoff less than the atmospheric cutoff of 1 GV typically peak (and therefore rise) earlier than those with higher cutoff rigidities. In contrast with P1, this suggests a source mechanism in which the acceleration time increases with rigidity. CME shock acceleration is a natural candidate for this.

6. Fluence. A generally accepted explanation for a double-pulse nature of GLEs is that it can be caused by propagation effects in the heliospheric magnetic field. Such an explanation only needs one acceleration mechanism, by implication the CME shock. An example of such a propagation effect is that P2 may be the reflection or back-scattering of P1 from a magnetic

barrier beyond 1 AU, as invoked by Bieber et al. (2004) for GLE 60. We contend this cannot be the case for GLE 69 because the number of solar cosmic rays returning towards the Sun in P2 is significantly greater than the number moving outwards in P1, only some tens of minutes previously. (Seen by integration of the directional intensities over the hemispheres away from, and towards the sun, over the duration of the pulses, after allowance for the direction of the HMF). That is, even 100% reflection of P1 is insufficient to explain the observed amplitude of P2, and an additional source of particles is necessary. We also note an early paper by Jokipii (1968) that questions the hypothesis of relatively rapid backscatter on theoretical grounds. In our view, the extra source of particles is the second population discussed in paragraph (1) above, whose anisotropic characteristics are strongly different from P1 because of the different injection points in the corona.

Items 1 to 6 above suggest different source mechanisms for the two pulses. The anisotropic, prompt nature, and the short duration of P1 naturally suggests that its source was the localized flare, with the more gradual, less anisotropic P2 being more likely produced by first-order Fermi acceleration in the more extended and more gradually developing CME shock.

7. Association with high-energy gamma rays. The above six arguments were based on the properties of the particle pulses alone. The association of P1 with the flare is strengthened by the presence of high-energy gamma rays. In Figure 10 of Paper 1 it was shown that there was >60 MeV gamma radiation present from the general position of the flare at 14°N, 61°W with which this GLE is associated. These gamma rays emanate from the decay of pions that are produced in reactions of the high-energy protons with dense matter. The leading edge of this gamma radiation had the same rate of increase as that of pulse P1. This association suggests that P1 was accelerated low in the corona, and therefore likely in the flare itself. A problem is, however, that the gamma peak occurred 7 to 8 minutes earlier than the particle peak. This delay implies that the particles traveled a path length of $\sim$1.7 AU in the heliosphere before being observed at Earth. This is significantly longer than the path length of $\sim$1.2 AU expected from propagation along the Parker spiral. The Milagro studies reported in this series by Ryan et al. (2010) indicate that the maximum possible path length for particles in P1 is 1.5 AU, and that the leading edge of P1 can not be satisfactorily associated with these high-energy gamma rays.

This timing argument involves the details of (a) the form of the leading edges of the respective pulse and the correct identification of the start times, and (b) the signatures in the radio and X-ray signals that indicate when open field lines were present for the first time to release the accelerated particles. It leads to timing uncertainties of perhaps $\pm$ 1 min., and it does not fully resolve the association of P1 with the flare. We therefore base our arguments for two source mechanisms mainly on the properties of the GLE itself.

3 The GLEs of Solar Cycle 23

GLE 69 was so large, and it had such a prompt first peak that it serves as an excellent example to search for other GLEs with similar properties, in particular for those with double-peak structures. We thus systematically studied the time structure of all the GLEs of SC 23, to identify more of these events. The current study is limited to SC 23 partly because these most recent events are the best observed ones.

The results of this survey are summarized in Table 1. The table was compiled from a graphical analysis of each GLE, similar to what was done in Fig. 1 for GLE 69. We stress that we included all the available NM data to ensure that no effect was missed.

Table 1 Ground level enhancements in solar cycle 23

GLE No	Date	Single or 1st Pulse			2nd Pulse (when seen)			Incr. rate %/min; Rise time min.	Onset disp min.	P_{max} GV	Flare			CME start/ height
		Start	Max	%	Start	Max	%				Lat. Lon.	X-ray imp.	X-ray Onset	
55	1997	12:31	13:28	18				0.4	0	Lmks	S18	X9.4	11:49?	11:39
	1106	Many	San2	San2				57		4.0	W63			5.2
56	1998	14:00	14:09	10.4				2.2	0	1.88	S15	X1.1	13:31	13:32
	0502	Many	Gsby	Gsby				9		Hbrt	W15			3.3
57	1998	?	?	0						–	S11	X2.7	07:59	07:55
	0506										W65			3.8
58	1998	22:42	22:53	3				0.06	0	<1 GV	N35	X1.0	21:50	?
	0824	Sane	Sane	Sane				11			E09			
59	2000	10:31	10:42	83				3.2	6	4.0	N22	X5.7	10:03	10:25
	0714	Apty	Thul	San2				9		Lmks	W07			1.4
60	2001	13:55	14:11	181	14:05	14:58	81	17	8	6.69	S20	X14.	13:19	13:35
	0415	Calg	Pwnk	Sopo	Caps	Caps	Caps	16		Aatb	W85			3.3
61	2001	02:36	03:13	19	03:23	03:35	26	0.3	70	3.66	S23	?	00:14?	02:11
	0418	Tera	Tera	McM	Sopo	Sopo	Sopo	37		Irkt	W117	?		5.9
62	2001	16:40	17:43	5				0.1	0	<1 GV	N06	X1.0	16:03	16:13
	1104	Tera	San2	San2				57			W18			8.0
63	2001	05:40	05:55	12				0.3	15	1.19	N08	M7.1	04:32	05:06
	1226	Apty	Apty	Sopo				15		Kerg	W54			4.2

Table 1 (*Continued*)

GLE No	Date	Single or 1st Pulse			2nd Pulse (when seen)			Incr. rate %/min; Rise time min.	Onset disp min.	P_{max} GV	Flare			CME start/ height
		Start	Max	%	Start	Max	%				Lat. Lon.	X-ray imp.	X-ray Onset	
64	2002	01:24	01:37	4				0.3	5	1.7	S02	X3.1	00:49	00:59
	0824	Kerg	Kerg	Kerg				13		Yktk	W81			3.6
65	2003	11:12	11:17	24	11:12	11:53	45	5.5	20	4	S20	X17	11:00	11:07
	1028	Nrlk	Nrlk	Nrlk	McM	McM	McM	5		Lmks	E02			3.9
66	2003	21:01	21:15	35	23:00	24:00	15	3.3	0	6.69	S19	X10	20:37	20:43
	1029	Many	Sopo	Sopo	Many	Many	Nain	14		Aatb	W09			8.7
67	2003	17:30	17:52	39				2.5	10	4.00	S18	X8.3	17:18	17:19
	1102	Sopo	Sopo	Sopo				22		Lmks	W59			3.0
68	2005	?	?	Very							N14	X3.8	09:52	09:43
	0117			Small							W25			3.2
69	2005	06:49	06:54	8000	06:53	07:06	306	1600	10	14.1	N14	X7.1	06:39	06:33
	0120	Sopo	Sopo	Sopo	Apty	Invk	Invk	5		Tibet	W61			4.0
70	2006	02:50	2:57	68	03:07	03:28	55	13	13	4.61	S06	X3.4	02:17	02:25
	1213	Many	Mwsn	Mwsn	Thul	Barb	Mwsn	7		Jung	W23			4.2

Aatb = Alma Ata B, Apty = Apatity, Barb = Batrentzburg, Calg = Calgary, Caps = Cape Schmidt, Gsby = Goose Bay, Hbrt = Hobart, Invk = Inuvik, Irkt = Irkutsk, Jung = Junfraujoch, Kerg = Kerguelen, Lmsk = Lomnicki Stit, McM = McMurdo, Mwsn = Mawson, Nrlk = Norilsk, Pwnk = Peawanuk, Sane = Sanae, San2 = Sanae NMD, Sopo = South Pole, Thul = Thule, Tera = Terre Adelie, Yktk = Yakutsk

South Pole and Sanae are not corrected for altitude

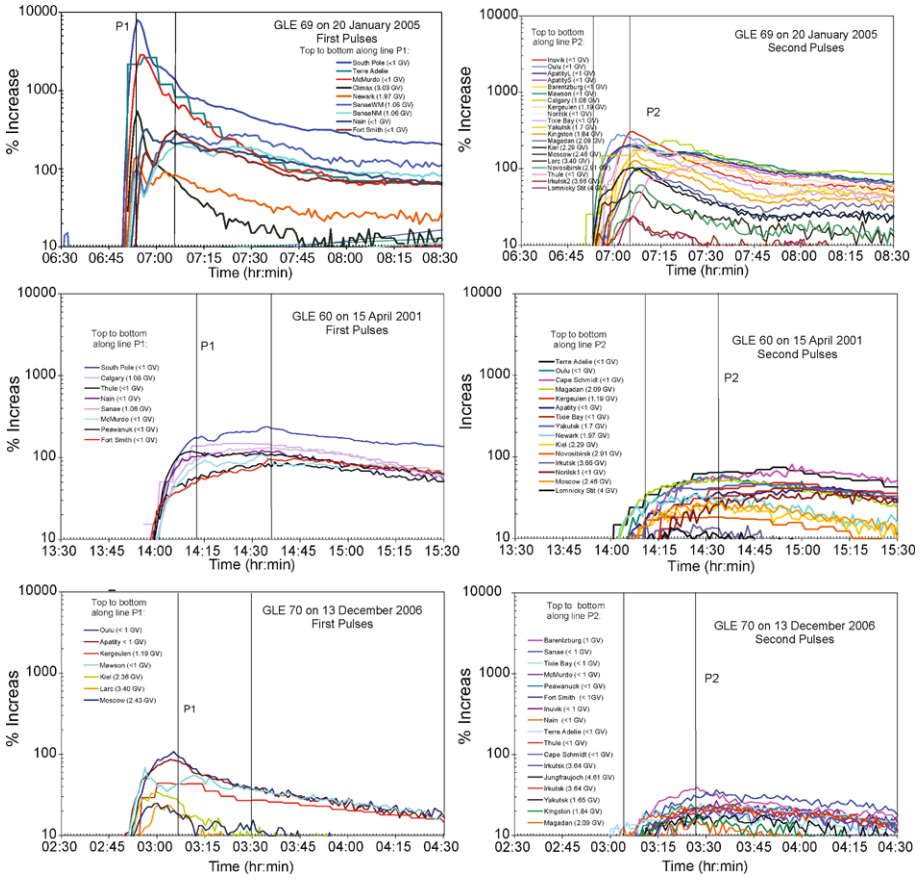

Fig. 2 Ground Level Enhancements 69 (*top*), 60 (*middle*) and 70 (*bottom*) in the same format as in Fig. 1, and all on the same scale to aid visual comparison of the size, rate of increase, and duration of each event. These are the only three out of 16 GLEs of solar cycle 23 that show the double pulse structure first identified in GLE 69 by McCracken et al. (2008)

For each event the start time, the time of maximum, and the amplitude is given, together with the NMs on which they were seen. If these features are similar for several NMs, they are listed as "many". The column "onset dispersion" lists the time difference between the earliest and latest onset, because we noted in Paper 1 that there should be a significant difference in onset times if there are multiple pulses. (Notice that this is not the dispersion within each of the peaks as discussed for GLE 69 above, but the total time interval from the earliest P1 to the latest P2.) The column P_{max} gives the name of the NM with the highest cutoff rigidity that saw the event. This is a coarse indication of the hardness of the spectrum. The column with increase rate (in %/min.) and rise time (in min.) gives two indicators of the promptness of the event.

The most outstanding feature of the table is the prompt nature of GLE 69. (Although it was large, its magnitude was not outstanding, because it was only second to GLE 05 of 23 February 1956.) Its rate of increase, measured on the leading edge of P1, was ≈1600%/min. and its rise-time to maximum only ≈5 min. The next two in the list had a rate of increase of ≈17%/min. and a rise time of 16 min. for GLE 60, and ≈13 %/min. and 7 min. for GLE

70. We have not yet analyzed events before GLE 55 in great detail. However, from several published figures of GLE 05 on 23 February 1956, e.g. Vashenyuk et al. (2007), it appears that its rate of increase was "only" ≈300%/min., i.e much smaller than for GLE 69. For GLE 69 the peak width at half maximum was only ≈4 min. while for GLE 05 it was ≈25 min. Hence, P1 of GLE 69 seems to be the fastest and narrowest GLE pulse ever recorded.

Of the 16 GLEs in the list, six suggest a double-pulse nature. However, only three of these, numbers 60, 69, and 70 show the clear double-pulse feature defined by GLE 69. GLEs 61 and 66 do not qualify for double-pulses because the onset times of the two pulses differ by one and two hours respectively, which suggests that the two pulses were not from a flare and a CME associated with the same event. GLE 65 is also excluded because Norilsk was the only station to record the first pulse, and the fact that its associated active region was at 2°E raises questions about whether this could have been an increase along a well-connected field line.

Figure 2 shows these three double-pulse GLEs of solar cycle 23, all on the same time and intensity scales to easily compare their amplitude, rise and decay rates, and time dispersions. GLEs 60 of 15 April 2001, and GLE 70 of 13 December 2006 have been studied extensively, e.g. by McCracken et al. (2008), Timashkov et al. (2007), Vashenyuk et al. (2007), Bieber et al. (2007), Grigoryev et al. (2007), Balabin et al. (2007) and Abbasi et al. (2008). They are much smaller than GLE 69, with peak increases of only ∼200% (GLE 60), and ∼100% (GLE 70), as compared to 8000% for GLE 69. The features that are clearly similar to those of GLE 69 are (a) a time delay of several minutes between the onset of the two pulses, (b) a similar delay in their time of maximum, (c) only a few stations saw P1, indicating that these pulses were strongly anisotropic, (d) the fluence in P2 was larger than in P1, although this is marginal for GLE 60, and (e) small velocity dispersion in the onset of P1, but large in the case of P2. Features that are different from those in GLE 69 are (a) P1 of GLE 70 is significantly structured. Oulu and Apatity have 'normal' peaks, but Mawson shows a substructure of two peaks, which may also explain the flat response of Kerguelen (which is only shown in 5-min. resolution). It is not clear what the origin of this structure is, but it seems more natural that such structure is associated with the small-scale, fast-changing flare origin, than with the more extended, slower-changing shock. (b) P1 of GLE 60 is so gradual that it is hardly distinct in form from P2. In this case the two most significant differences between the two pulses are that P1 has a smaller velocity dispersion in the onset times, and its increase rate is faster.

At this point we mention that another explanation, by Saiz et al. (2008), for the double pulses is that they arrive at Earth via the opposite legs of an extended, closed magnetic loop. This does, however, not address why in all three cases the majority of the particles (i.e. the larger fluence in P2) comes via the longer of the two paths.

4 Flare and CME Associations

Finally, we compare the GLEs with some of the available flare and CME information (Gopalswamy et al. 2010). This information in Table 1 was supplied as part of the Co-ordinated Data Analysis Workshops (CDAW) in 2009. The flare information reveals the well-known association with western flares, which should be well-connected to Earth via the HMF, with only three exceptions (58, 61, 65) that fall outside the range 0°W–90°W. However, a finer association of GLE magnitude an promptness with flare position does not yield a clear pattern.

The same is true for the association with flare magnitude in terms of X-ray importance. There were, for instance, five flares that were stronger than the one of 20 January 2005. We

Table 2 Time difference (min.) between GLE onset and estimated CME lift-off

GLE	55	56	59	60	61	62	63	64	65	66	67	69	70
ΔT	52	28	6	20	25	27	34	25	5	18	11	16	25

note, however, that of the four largest events in Table 1, the three west of 23°W (60, 69 and 70) exhibit double peak structures, while GLE 59, which was associated with a flare at 1°W, does not. This supports the result in Paper 1 that a double-peak structure is observed for the majority of large GLEs associated with solar activity to the west of ∼25°W. At the very least, GLE magnitude should be a combined function of activity level and the degree of magnetic connectedness between the source and Earth, and the latter is generally unknown in detail.

The quoted CME start times in the last column of the table are the probable "lift-off" times from the sun, extrapolated backwards from the observed CME speed and the first observation by the LASCO coronagraph. The height, in solar radii, when the CME was first seen is given as the second number. For typical numbers of CME speed of 2000 km/s and the first point of observation at 4 solar radii, this correction from first observation time to lift-off time amounts to ∼25 min., and this introduces a significant timing uncertainty.

Table 2 lists the time difference between this estimated time of CME lift-off and the time of earliest onset of each of the GLEs (3rd column, Table 1). One of the central issues to differentiate between CME and flare (or other) acceleration is whether there is sufficient time for the CME to form, to develop a bow shock, and to accelerate particles into a power law up to a few GeV. As described earlier, for first-order Fermi (or shock) acceleration, this acceleration time scale is proportional to rigidity, and it is of the order of 1 hr at 1 GV. Hence the available times in Table 2 are uncomfortably short for CME acceleration. We note, however, that this time scale may be significantly decreased through self-excitation of waves, as was recently calculated by Ng and Reames (2008) for a parallel shock. In addition, acceleration at a perpendicular shock could be even faster, e.g. Tylka et al. (2005) and references therein, and might conceivably start lower in the atmosphere. For the case of GLE 69 the CDAW concluded that, given the large uncertainties, a CME shock acceleration source for P1 could not be excluded on the basis of timing.

Finally, charge state and composition of solar energetic particle events are accepted diagnostic tools to identify the source of these particles, e.g. Labrador et al. (2005) and Mewaldt et al. (2007). We are, however, not aware of these measurements extending to GLE energies, or differentiating between P1 and P2 in the double-pulse events.

5 Summary and Conclusion

The complete list of 16 GLEs observed during solar cycle 23 reveals that three of these events, numbers 60, 69, and 70 had the well-defined double-pulse feature of GLE 69 of 20 January 2005, described in McCracken et al. (2008). These three were associated with western flares, and hence should have been well-connected via the HMF to Earth. P1 of GLE 69 had by far the fastest rise-time and shortest duration on the list, even when it is compared to the largest GLE of 23 February 1956.

The common properties of the three double-pulsed GLEs are (a) a large, prompt, anisotropic first pulse, followed by a smaller, more gradual, less anisotropic second pulse, (b) there is little time dispersion in the onset and rise to maximum in P1, but it is large in P2, and (c) although P1 is generally larger than P2, the fluence in P2 is larger than in P1.

This discounts a previous hypothesis that P2 is a remainder of P1 that is back-reflected from positions beyond 1 AU to Earth due to increased scattering.

On this basis of these properties we deduced that the flare and the CME shock are natural candidates to produce P1 and P2 respectively.

This hypothesis is strengthened by the presence of gamma radiation from the decay of pions at the time of P1, which indicates that it was produced low in the corona. A vulnerable aspect is, however, that the flare acceleration of P1 in GLE 69 implies a path length of up to 1.7 AU in the heliosphere, which is considerably longer than the ∼1.2 AU expected from propagation along the Parker spiral. However, there are no observations that indicate that during this disturbed period the length of the field line was the minimum value determined by the Parker spiral.

Finally, detailed associations between GLE magnitude and flare position, importance, and CME dynamics do not yield a straightforward answer as to the origin of the two pulses. The strongest evidence for a double acceleration mechanism is in the nature of the pulses themselves.

Acknowledgements We acknowledge the use of data of over 50 NMs, conveniently available in a centralized data base. We are greatly indebted to M.A. Shea and D.F. Smart who established this data base of GLE reports over many years, to M.L. Duldig who took it over form them, and to E.A. Eroshenko who currently maintains it. The flare and CME information used in Table 1 was supplied by N. Gopalswamy as part of the CDAW.

References

R. Abbasi et al. (IceTop). Astrophys. J. **659**, L65 (2008)
Y.V. Balabin, B.B. Gvozdevsky, E.V. Vashenyuk et al., in *Proc. 30th ICRC*, vol. 1, p. 257 (2007)
J.W. Bieber, W. Dröge, P. Evenson, R. Pyle, D. Ruffolo, U. Pinsook, P. Tooprakai, M. Rujiwarodom, T. Khumlumlert, S. Krucker, Astrophys. J. **567**, 622 (2002)
J.W. Bieber, P. Evenson, W. Dröge, R. Pyle, D. Ruffolo, M. Rujiwarodom, P. Tooprakai, T. Khumlumlert, Astrophys. J. Lett. **601**, L103 (2004)
J.W. Bieber, J.M. Clem, P.A. Evenson et al., in *Proc. 30th ICRC*, vol. 1, p. 229 (2007)
R.A. Caballero-Lopez, H. Moraal, F.B. McDonald, J. Geophys. Res. **109**, A05105 (2004). doi:10.1029/2003JA010358
E.W. Cliver, in *Proc. IAU Symp.*, vol. 257 (Cambridge Univ. Press, Cambridge, 2008), p. 401
N. Gopalswamy, H. Xie, S. Yashiro, I. Usoskin, Indian J. Radio Space Phys. **39**(5), 240–248 (2010)
V.G. Grigoryev, S.A. Starodubtsev, P.A. Krivoshapkin et al., in *Proc. 30th ICRC*, vol. 1, p. 233 (2007)
J.R. Jokipii, Astrophys. J. **152**, 997 (1968)
A.W. Labrador, R.A. Leske, R.A. Mewaldt, E.C. Stone, T.T. von Rosenvinge, in *Proc. 29th ICRC*, vol. 1, p. 99 (2005)
K.G. McCracken, H. Moraal, P.H. Stoker, J. Geophys. Res. **113**, A12101 (2008). doi:10.1029/2007JA012829
R.A. Mewaldt, C.M.S. Cohen, G.M. Mason, A.C. Cummings, M.I. Desai, R.A. Leske, J. Raines, E.C. Stone, M.E. Wiedenbeck, T.T. von Rosenvinge, T.H. Zurbuchen, Space Sci. Rev. **130**, 207 (2007). doi:10.1007/s11214-007-9187-1
H. Moraal, J.P.L. Reinecke, K.G. McCracken, in *Proc. 31st ICRC*, p. 1553 (2009)
C.K. Ng, D.V. Reames, Astrophys. J. **686**, L123 (2008)
J. Ryan et al., Space. Sci. Rev. (2010, this issue)
A. Saiz, D. Ruffolo, J.W. Bieber, P. Evenson, R. Pyle, Astrophys. J. **672**, 650 (2008)
D.A. Timashkov, Yu.V. Balabin, V.V. Borog et al., in *Proc. 30th ICRC*, vol. 1, p. 209 (2007)
A.J. Tylka et al., Astrophys. J. **625**, 474 (2005)
E.V. Vashenyuk, G.A. Bazilevskaya, Y.V. Balabin et al., in *Proc. 30th ICRC*, vol. 1, p. 221 (2007)
T.T. Von Rosenvinge, H.V. Cane, in *Geophysical Monograph*, vol. 165, ed. by N. Gopalswamy et al. (American Geophysical Union, Washington, 2006), p. 103